Prediction of effective reaction rates in catalytic systems of multiple reactions using one-dimensional models

M.J. Taulamet[a,b], N.J. Mariani[a,b], O.M. Martínez[a,b], G.F. Barreto[a,b,*]

[a] PROIRQ, Departamento de Ingeniería Química, Facultad de Ingeniería, Universidad Nacional de La Plata, La Plata, Argentina
[b] Centro de Investigación y Desarrollo en Ciencias Aplicadas "Dr. J. J. Ronco", (CINDECA) CONICET – UNLP – CCT La Plata, Calle 47 Nº. 257, CP B1900AJK La Plata, Argentina

ABSTRACT

In this work two one-dimensional (1D) models are used to approximate the catalytic behavior of three-dimensional (3D) shaped pellets. One of the 1D models employs a single parameter and is identified as Generalized Cylinder (1D-GC), while the second model, named Variable Diffusivity model (1D-VD), makes use of three parameters. Both models have been introduced in previous contributions and their performances were successfully tested for single catalytic reactions. A conventional system of two first order reactions in series and the process of selective hydrogenation of butadiene in the presence of 1-butene that shows strong inhibition effects are considered. The pellet shapes for which the largest errors were detected when using the 1D models in the cases of a single reaction were selected for this study. It was found that the use of the 1D-GC model leads to errors in the estimation of the effective reaction rate of up to around 7% for the first-order series-reaction system and up to 20% for the hydrogenation selective process. In contrast, the 1D-VD model can be used with a maximum error of the order of 1% for the first-order series-reaction system and about 4% for the selective hydrogenation system.

1. Introduction

The reaction–diffusion equations inside non-spherical catalytic pellets should be expressed in two (2D) or, in general, three (3D) spatial dimensions. An analytical solution will be possible only for linear kinetic and flux models and for isothermal conditions. It follows that most frequently a numerical solution will be needed for solving the conservation equations. This task is computationally accessible for a limited number of operating conditions. However, if the optimization of a reactor is to be addressed, and in particular when dealing with systems involving a set of reactions, it is evident that the demand for computation time will grow significantly, since the calculations must be repeated in the order of thousands of times. Therefore, it is highly desirable to avoid numerical calculations involving 2 or 3 spatial dimensions.

Aris [2] presented a simple approach to reduce 2D or 3D problems to a one-dimensional (1D) problem. It is based on the fact that at high enough values of the Thiele modulus (ϕ), the effectiveness factor for a single reaction does not depend on the shape of the catalytic pellet, but only on the ratio of the volume to its external surface ($\ell = V_p/S_p$). In order to carry out approximate evaluations of low and intermediate

values of ϕ, a simple geometry (*e.g.*, a slab) having the same value of ℓ as the actual pellet can be adopted. The expected precision using this approximation is of the order of 20% for a single reaction and with relatively simple kinetic expressions.

Datta and Leung [5] proposed a more convenient 1D model, called the generalized cylinder (1D-GC), in which diffusion proceeds along a single direction z of a hypothetical catalytic body with a cross-section variable according to z^σ. The definition of the parameter σ (called the shape factor) was extensively discussed and systematized by Mariani et al. [10,11,12,13], who showed the aptitude of the 1D-GC to approximate accurately the effective reaction rates for single reactions with simple kinetic expressions.

However, it was found that the 1D-GC model may lead to significant errors for some pellet shapes when the relationships between the geometric dimensions reach critical values [16] or when the reaction is accelerated inside the catalyst, either by thermal or inhibition effects [14]. In order to recover a high level of precision, a new three-parameter one-dimensional model, called variable diffusivity model (1D-VD), was proposed. The three parameters are evaluated by satisfying simultaneously the behavior of the actual pellet at high and low reaction rates. The 1D-VD model guarantees an accuracy better than 2%

Nomenclature

1-BE	1-butene
a, b, c	geometric parameters from pellets in Table 1 [m]
b^*	dimensionless pellet height [–]
BA	n-butane
BD	1,3-butadiene
BY	1-butyne
C_k	molar concentration of species k [mol m^{-3}]
D	effective diffusivity of the limiting reactant [m^2 s^{-1}]
D_k	effective diffusivity of the species k [m^2 s^{-1}]
$_i(z)$	coefficient for the effective diffusivity in the 1D-VD model, defined in Eq. (6) [–]
H	pellet height [m]
k_{cj}	specific kinetic coefficient of the reaction j, Eqs. (8a) and (8b) [s^{-1}]
k_j	specific kinetic coefficient of the reaction j, Eqs. (11a) and (11b) [mol m^{-3} s^{-1}]
K_k	equilibrium adsorption constant of the species k [–]
ℓ	V_P/S_P; characteristic length of the pellet [m]
L	diffusion length for 1D models [m]
r_j	rate of the reaction j [mol m^{-3} s^{-1}]
r_{ref}	reference rate of reaction defined in Eq. (13c)
S_p	external surface area of the pellet accessible to reactants [m^2]
V_p	pellet volume [m^3]

y_k	mole fraction of the species k [–]
z'	spatial coordinate for 1D models [–]
z	dimensionless coordinate for the 1D models, z'/L [–]

Greek Letters

$\varepsilon_1, \varepsilon_2$	relative errors in the predictions of effective reaction rates defined in Eqs. (13a) and (13b), respectively
$\delta_{j,GC}$	relative difference in the predictions from the 1D-GCγ and 1D-GCΓ models for the reaction j, defined in Eqs. (18a) and (18b) [–]
π_k	consumption/generation rate of the species k [mol m^{-3} s^{-1}]
ϕ_j	Thiele modulus for the reaction j [–]
γ, Γ, β	geometric parameters of the actual pellet [–]
σ	shape factor; parameter of the 1D-GC model, defined in Eqs. (4) and (5) for the 1D-GCγ and 1D-GCΓ alternatives, respectively [–]
ψ_1, ψ_2, α	parameters of the 1D-VD model in Eq. (6) [–]

Superscripts and Subscripts

s	value at the pellet surface (S_P)
eff	effective value
max	maximum value

when used for isothermal first-order kinetics and a wide set of catalytic pellet shapes and their geometric relationships [16]. On the other hand, Mariani et al. [14] analyzed the effect of kinetic expressions on the accuracy of 1D models, extending the analysis to the limit where multiple stationary states arise. It turned out that when the 1D-GC model is used, errors can grow up to 40%, while the 1D-VD model allows keeping the maximum deviations below 10%, for the most critical cases.

Some other contributions have also addressed the problem of diffusion and a single reaction in 2D or 3D pellet shapes by using a 1D approximation, as those of Miller and Lee [15], Burghardt and Kubaczka [4], Wijngaarden et al. [23], Papadias et al. [18], Buffham [3] and Lopes et al. [9]. As discussed in our previous works [7,8,10–14], those contributions do not present general criterions to fix the parameters of the 1D model to the actual shape of the catalyst or are devoted to specific cases as for thin catalytic coatings [9] or 2D shapes [18]. The recent presentation of Schweitzer et al. [21] also deals with 2D shapes, as arise from long multi-lobe cylinders.

The summarized findings provide a solid basis for asserting that 1D-models (in particular, the 1D-VD model) allow for a suitable representation of the behavior of single reactions taking place in actual 3D catalytic pellets. However, it is very common in industrial processes to find multiple reaction systems [17]. Some authors tested 1D approximations to a case study of multiple reactions. For example, Piña et al. [20] and more recently Piña and Borio [19] studied the steam reforming process considering the three main catalytic reactions on a seven-holed pellet with convex ends (Haldor Topsoe R-67-7H). The actual geometry was replaced by an equivalent 1D geometry defined as an infinite hollow cylinder with the inner radius equals to that of the actual holes and an external radius defined to match the same value of ℓ as the actual pellet. Dixon and Cresswell [6] tried an equivalent slab, an infinite cylinder and a sphere to simulate the behavior of a finite hollow (Raschig ring) and a solid cylinders for a given consecutive-parallel reaction scheme. It was concluded that the equivalent infinite cylinder allows reaching the more accurate estimations of the effectiveness factors. The works summarized above exemplify that previous contributions deal with specific cases of pellet shapes and reaction systems,

and the 1D approximation was chosen to fit such cases, but without trying to systematize a general procedure to reduce the dimensionality.

The objective of this work is to carry out an exhaustive analysis of the behavior of the 1D-GC and 1D-VD models for two selected cases: a system of first-order series reactions and the selective hydrogenation process of butadiene in the presence of 1-butene, in both cases under isothermal conditions, for a representative set of pellet shapes commercially employed. These examples were chosen because they lead to the existence of maximums in the rate of some of the reactions, inside the catalytic pellet. This poses a challenging feature for the 1D approximations, since the relevant maximum reaction rate cannot be identified beforehand and its magnitude and location will depend on properly predicting the evolution of the composition inside the pellet.

2. 1D models and pellet shapes

The mass conservation equations for the diffusion-reaction problem in a pellet of any shape, assuming steady state conditions, uniform catalytic activity and fluxes described by the Fick law with uniform effective diffusivity can be written according to Eqs. (1).

$$D_k \mathscr{L}(C_k) = \ell^2 \pi_k, \text{ in } V_p \tag{1a}$$

$$C_k = C_{k,S}, \text{ on } S_p \tag{1b}$$

where $\mathscr{L}$ is the Laplace operator with dimensionless coordinates ($x_i = x'_i/\ell$), C_k is the molar concentration of species k and $C_{k,S}$ the uniform value on S_p. The consumption rate π_k is related to the reaction rates r_j as $\pi_k = \sum_{j=1}^{R} \nu_{jk} r_j$, where ν_{jk} are the stoichiometric coefficients.

The effective reaction and consumption rates are defined as

$$r_j^{eff} = \frac{1}{V_p} \int_{V_P} r_j dV \tag{2a}$$

$$\pi_k^{eff} = \sum_{j=1}^{R} \nu_{jk} r_j^{eff} \tag{2b}$$

The 1D-GC model is based on catalytic body with variable cross-section $S(z) = S_p z^\sigma$, where the dimensional coordinate $z = z'/L$ defines

the direction of the mass (and eventually heat) fluxes, between z = 1 (the external surface) and z = 0 (the apex of the body). The geometric parameter of the model is the exponent σ, while the diffusion length L can be written in terms of V_p as $L\, S_p/(1 + \sigma) = V_p$. The values of V_p and S_p are taken to be the same as those of the actual pellet. In this way, the model keeps the value of the characteristic length ℓ, and L can be re-written as $L = \ell(\sigma + 1)$. For the 1D-GC model the conservation equations become:

$$D_k z^{-\sigma} \frac{d}{dz}\left(z^\sigma \frac{dC_k}{dz}\right) = (1 + \sigma)^2 \ell^2 \pi_k \tag{3a}$$

$$dC_k/dz = 0, \text{ at } z = 0 \tag{3b}$$

$$C_k = C_{k,S}, \text{ at } z = 1 \tag{3c}$$

When σ = 0, 1, 2 the model reduces to a slab, an infinitely long circular cylinder and a sphere, respectively. For using the 1D-GC model to approximate the behavior of a given 3D pellet shape, the target is that the effective reaction rates, as defined in Eq. (2a), can be evaluated by the model as closely as possible as the actual values in the 3D pellet. To this end, the value of the model parameter σ should be chosen according to a certain geometrical criterion. The "geometrical" restriction is highly desirable, in practice, to associate σ to the geometry of the actual 3D pellet, irrespective of kinetic expressions and operating conditions.

Two basic criterions were used and tested in previous contributions for single reactions [7,8,10–14,16].

One of them is based on expanding the ratio (r^{eff}/r_S) (r_S is the reaction rate at the external surface conditions) in powers of the square of the Thiele modulus, $\phi^2 = \ell^2 r_S/(DC_S)$ for a given pellet shape, as originally proposed by Mariani et al. [11]. The zero-order term of the series is 1 and the second and third terms are proportional to factors γ and β that depend strictly on the shape of the pellet [11]. The values of γ and β are evaluated from the solution of a Poisson equation on the pellet volume. By noting that ϕ^2 will be the same for 1D-GC model and for the actual 3D pellet, it is then required that the 1D-GC model renders the same value of γ as the actual pellet. For the 1D-GC model, a simple relation arise, $\gamma_{1D\text{-}GC} = (1 + \sigma)/(3 + \sigma)$. Therefore, the criterion to evaluate σ from matching the same value γ as that of the actual pellet is expressed by

$$\sigma_\gamma = (3\gamma - 1)/(1 - \gamma), \tag{4}$$

where the suffix γ for σ_γ is used to recall the criterion employed and γ is the value for the actual pellet. The formulation to calculate γ for any pellet shape is detailed in Mariani et al. [11], along with close approximations for some specific pellet shapes. Extensions to calculate γ, and also β, for a spatial distribution of catalytic activity and transport models other than Fick law are discussed by Mocciaro et al. [16]. For an abbreviate presentation just dealing with the problem posed in Eqs. (1), the reader can consult the work of Mariani et al. [14]. It is stressed that the task for a given particle shape should be performed once for all.

It becomes evident that using Eq. (4) for the parameter σ of the 1D-GC model will render a good approximation for r^{eff} provided that ϕ^2 is effectively low. If ϕ^2 is very high, the result for r^{eff} will also be accurate, as it will be proportional to $(1/\phi)$ for both, 1D-GC model and actual pellet. Deviations, therefore, will be circumscribed to intermediate values of φ.

The second criterion to fix σ arises by expanding (r^{eff}/r_S) in powers of $(1/\phi)$. The first order term corresponds to the limiting value just mentioned above and the second term is proportional to a geometrical factor Γ. This factor can be written as the sum of two contributions, $\Gamma = \underset{\smile}{\Gamma} + \widehat{\Gamma}$, where $\underset{\smile}{\Gamma}$ can be explicitly expressed in terms of the curvature of the smooth sectors on the external surface of the pellet [7] and $\widehat{\Gamma}$ depends on the included angle of the (eventual) edges formed from the intersection of smooth sectors and slightly on the shape of the reaction rate law [8]. An explicit approximation $\widehat{\Gamma}$ was given by Keegan et al. [8]. For the 1D-GC model, $\Gamma_{1D\text{-}GC} = \sigma/(1 + \sigma)$. Then, the alternative

criterion to evaluate σ is fitting the Γ value of the 1D-GC model to the value of the actual pellet:

$$\sigma_\Gamma = \Gamma/(1 - \Gamma) \tag{5}$$

where Γ is the value for the actual pellet. Using Eq. (5), the 1D-GC model will be capable to provide a precise approximation to r^{eff} for high and moderately high values of φ, while the limiting value ($r^{eff}/r_S) \to 1$ as $\phi \to 0$ will be also matched. Again, deviations will be found for intermediate values of φ, although displaced to lower values of φ with respect to the use of Eq. (4). The formulation to evaluate Γ was summarized by Mocciaro et al. [16] and just for the problem defined by Eqs. (1) by Mariani et al. [14].

For multiple reaction systems, the set r_j^{eff} can be expanded in a similar way as described for a single reaction. The meaning and values of the parameters γ, β, Γ remain unaltered, for a given pellet shape. The same applies for $\widehat{\Gamma}$ in the case of first order reaction rates [22]. Following the results for a single reaction, it can be expected with confidence that using the value of $\widehat{\Gamma}$ for a first order reaction will be suitable in most instances. This fact has been checked to be true from the results of the selective hydrogenation example undertaken in this work.

The 3-parameter 1D-VD model introduced by Mocciaro et al. [16] assumes that reactions take place in a slab with half-thickness defined by the value of ℓ corresponding to the actual pellet. The pellet-shape effect is accounted for by assuming that the transport parameters of the species depend on the dimensionless spatial coordinate z = z′/L (z = 0 at the middle plane of the slab). For the Fick model used here:

$$\mathscr{D}_k(z) = D_k \exp[\psi_1(1-z) + \psi_2(1-z)^\alpha] \tag{6}$$

where ψ_1, ψ_2 and α are parameters defined in such a way as to satisfy the values of the geometrical parameters γ, β and Γ of the actual pellet, as explained by Mocciaro et al. [16].

The mass conservation equations, according to the 1D-VD are:

$$d[\mathscr{D}_k(z)dC_k/dz]/dz = \ell^2 \pi_k \tag{7a}$$

$$dC_k/dz = 0 \text{ at } z = 0 \tag{7b}$$
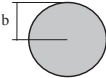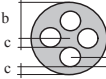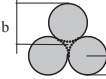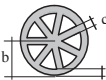
$$C_k = C_{k,S} \text{ at } z = 1 \tag{7c}$$

It should be remarked that for a prompt account on the evaluation of the actual 3D pellet geometrical parameters (γ, β and Γ) and the 1D-DV model parameters (ψ_1, ψ_2 and α), the reader is advised to consult the work of Mariani et al. [14].

Four shapes of the catalytic pellet were selected for the purpose of this contribution, which are illustrated in Table 1 along with the specific aspect ratios, which were taken from catalogues of commercially available pellets. The solid cylinder is a very common shape and was chosen as a standard. The selective hydrogenation example undertaken

Table 1
Shape of the cross-sections and geometric aspect ratios for the 3D pellet considered in this study ($b^* = b/H$, H is the height of the cylinder). The expressions to evaluate the geometric parameter Γ are also included (A_{CS}: cross-section area).

Pellet	Cross-section	Dimensions	($\Gamma A_{CS}/\ell^2$)
Solid cylinder		$b^* = 0.59, 2.5$	$32b^* + 2\pi$
4-holed ring		$a/b = 0.273$ $c/b = 0.227$ $b^* = 0.55$	$32b^*(1 + 4a/b) - 6\pi$
Trilobe		$a/b = \frac{\sqrt{3}}{2+\sqrt{3}}$ $b^* = 0.86$	$80b^*(a/b) + (5\pi - 6)$
Wagon wheel		$c/b = 0.2$ $b^* = 1.1$	$92.8b^* - 27.6$ (specific for $c/b = 0.2$)

in the following sections is carried out in trickle bed reactors, for which trilobe pellets are frequently employed. The two hollow cylinders (4-holed ring and wagon wheel) were chosen because these shapes were shown to introduce large deviations for r^{eff} when using 1D approximations for single reactions with highly non-linear kinetics [14]. Table 1 also include the expressions to evaluate Γ for different ratios $b^* = b/H$.

The values of the shape parameters γ, β and Γ for the pellet in Table 1 and the corresponding values of the 1D-model parameters are listed in Table 2, for the finite values of the ratio $b^* = b/H$ (Table 1) and also for $b^* = 0$ (infinitely long pellets). The latter set will be also employed in Section 4 because the 1D models frequently introduce larger deviations as $H \to \infty$ [16]. The solid cylinder is an exception, as the fluxes just follow a single (radial) direction when $H \to \infty$.

3. The reaction sets

The first example is defined by a couple of first-order irreversible series-reactions, $A \to B \to C$. Kinetics are then given by

$$r_1 = k_{c1}C_A, \tag{8a}$$

$$r_2 = k_{c2}C_B \tag{8b}$$

The Thiele moduli employed for these reactions are expressed as:

$$\phi_1^2 = \ell^2 k_{c1}/D_A \tag{9a}$$

$$\phi_2^2 = \ell^2 k_{c2}/D_B \tag{9b}$$

The solution of the general problem described by Eqs. (1), in terms of the profiles for $C_A/C_{A,S}$ and $C_B/C_{A,S}$, will depend on ϕ_1, ϕ_2 and the ratios $C_{B,S}/C_{A,S}$, D_B/D_A, apart from the specific features of the pellet shape. The ratios $r_j^{eff}/(k_{cj}C_{A,S})$ will depend on the same variables.

The second example concerns the catalytic hydrogenation of conjugate dienes and acetylenic compounds in mono-olefin rich streams. Pd is used as the main catalytic agent. Specifically for C4 cuts from thermal or catalytic cracking, 1,3 butadiene (BD) and some acetylenic species, *e.g.*, 1-butine (BY) should be eliminated to valorize the cut. The selectivity of the process is determined by the affinity of Pd to adsorb the polyunsaturated species that can cover completely the active sites, even at very low concentrations, thus avoiding the adsorption of the butene isomers (1-butene, 1BE; *cis* 2-butene, cBE; *trans* 2-butene, tBE) that otherwise would lead to their hydrogenation and hydro-isomerization. Such an inhibition effect is the main feature for choosing this process as a case study. A complete kinetic characterization in liquid phase of this catalytic reaction system on a commercial catalyst was carried out by Alves et al. [1]. Ten reactions involving the hydrogenation of BY, BD and of the hydrogenations and isomerizations of the butene isomers were kinetically identified. A significant simplification will be made here with the purpose of highlighting the inhibition effect on the performance of 1D-approximations, but without having to resort to a complex interpretation and description of the results. On one hand,

only the presence of BD has been retained, as acetylenics hydrogenate preferentially, thus leaving BD as the species responsible to avoid the reactions of the butene isomers. On the other hand, in spite that butene isomers compete for adsorption on the active sites, their adsorption strengths are similar. Therefore, the reactions of the isomers do not introduce any special feature. Only 1BE is retained, as the only product from BD hydrogenation and as the only olefin possible to be hydrogenated. In this way, the reactions finally considered in the present example are

$$BD + H_2 \overset{r_1}{\to} 1BE \tag{10a}$$

$$1BE + H_2 \overset{r_2}{\to} BA \tag{10b}$$

where BA stands for n-butane.

Following Alves et al. [1], the kinetic expressions can be written as:

$$r_1 = \left(\frac{K_{BD}}{K_{1BE}}\right)\frac{k_1 y_{BD} y_{H_2}}{DEN_{HC}} \tag{11a}$$

$$r_2 = \frac{k_2 y_{1BE} y_{H_2}}{DEN_{HC}} \tag{11b}$$

$$DEN_{HC} = \frac{\kappa}{K_{1BE}} + \left(\frac{K_{BD}}{K_{1BE}}\right)y_{BD} + y_{1BE} \tag{11c}$$

where the mole fractions are written as $y_k = C_k/C_T$ (k = BD, 1BE, H$_2$). K_{BD} and K_{1BE} are the adsorption constants of BD and 1BE and k_j (j = 1, 2) are the specific kinetic coefficients. The parameter κ in (11c) accounts for the adsorption of the saturated species (*e.g.* BA). In practice, the relation (κ/K_{1BE}) is very small as compared to the remaining contributions to DEN_{HC} for observable values of y_{BD} and y_{1BE}. For numerical evaluations, the value $\kappa/K_{1BE} = 10^{-4}$, was employed. Smaller values have been checked to leave the results virtually unchanged. The total molar concentration C_T can be regarded to remain constant in the course of the reactions. It should be noted that according to Alves et al. [1] the effective reaction order of H$_2$ in r_2 is slightly smaller than 1, but the simplification in (11b) is of no practical consequence for the purpose of the present work.

The underlying feature of reaction rate expressions is the role of the adsorption constant ratio (K_{BD}/K_{1BE}) that reaches values of around 1000 [1]. The inhibition exerted by the presence of BD upon the 1BE hydrogenation can be evaluated by the ratio $X = [(K_{BD}/K_{1BE})(y_{BD}/y_{1BE})]$. If $X \ll 1$ (e.g. when BD is absent), it is obtained from Eqs. (11b,c) that 1BE will react as a zero-order reaction with respect to itself, with a plateau value $r_2 = (k_2 y_{H2})$. Instead, if $X \gg 1$, $r_2 = (k_2 y_{H2})/X$. The zero-order feature is maintained, but r_2 is strongly depressed. Thus, with (K_{BD}/K_{1BE}) ~ 1000, even a value y_{BD} as low as $y_{BD} = y_{1BE}/100$ will cause r_2 to decrease by a factor of 10. On the other hand, provided y_{BD} is not very small, BD will also react closely as a zero order reaction, with a plateau value $r_1 = (k_1 y_{H2})$ (from Eqs. 11a,c).

The Thiele moduli related to the rates in Eqs. (11a,b) are defined as

Table 2
Shape-coefficients for the pellets in Table 1 and values of the parameters for the 1D-models.

	Parameter	Pellet							
		Solid cylinder		4-holed ring		Trilobe		Wagon wheel	
		$b^* = 0.59$	$b^* = 2.5$	$b^* = 0$	$b^* = 0.55$	$b^* = 0$	$b^* = 0.86$	$b^* = 0$	$b^* = 1.1$
3D-pellet	Γ	0.792	0.561	−0.241	0.164	0.377	0.732	−0.173	0.297
	γ	0.680	0.500	0.366	0.448	0.443	0.625	0.347	0.448
	β	0.690	0.334	0.185	0.290	0.255	0.566	0.180	0.307
1D-GC	σ_γ	3.246	0.996	0.157	0.622	0.595	2.333	0.063	0.624
	σ_Γ	3.809	1.275	−0.194	0.195	0.606	2.726	−0.148	0.423
1D-VD	α	3.140	4.835	5.229	5.795	4.156	3.356	12.375	11.302
	ψ_1	−1.584	−1.574	0.482	−0.327	−0.754	−1.463	0.346	−0.594
	ψ_2	−2.567	−2.476	−6.381	−5.970	−1.976	−2.483	−9.938	−8.497

$$\phi_1^2 = \ell^2 \frac{k_1}{D_{BD}C_T}\left(\frac{K_{BD}}{K_{1BE}}\right)Y_S \tag{12a}$$

$$\phi_2^2 = \ell^2 \frac{k_2}{D_{1BE}C_T}Y_S \tag{12b}$$

$$Y_S = \frac{y_{H2,S}}{\frac{\kappa}{K_{1BE}} + \left(\frac{K_{BD}}{K_{1BE}}\right)y_{BD,S} + y_{1BE,S}} \tag{12c}$$

The solution of Eqs. (1) will depend on several parameters: ϕ_1, ϕ_2, K_{BD}/K_{1BE}, $C_{1BE,S}/C_{BD,S}$, $C_{H2,S}/C_{BD,S}$, D_{1BE}/D_{BD}, D_{H2}/D_{BD}. To test the behavior of 1D models, some of them will be bounded or fix according to the actual levels of the variables involved (Section 4.2).

4. Results and discussion

The platform *Comsol Multiphysics*® was used to solve Eqs. (1) for the actual pellet and Eqs. (3) and (7) for the 1D-models. The size of the mesh for the numerical solution was adjusted to guarantee a precision of 0.1%.

At given values of the parameters, for both reaction sets defined in Section 3, the relative error in the estimation of r_1^{eff} (Eq. (2a)) introduced by the 1D models will be evaluated by

$$\varepsilon_1 = 100\frac{(r_1^{eff})_{1D}-r_1^{eff}}{r_1^{eff}} \tag{13a}$$

where r_1^{eff} is the value obtained with the actual pellet shape and the suffix 1D denotes the value from any of the 1D models: 1D-GCγ (using σ_γ, Eq. (4)), 1D-GCΓ (using σ_Γ, Eq. (5)) or 1D-VD. For the second reaction, the following measure of error will be used:

$$\varepsilon_2 = 100\frac{(r_2^{eff})_{1D}-r_2^{eff}}{r_{ref}^{eff}} \tag{13b}$$

$$r_{ref} = \max\{r_2^{eff}, \pi_B^{eff}\} \tag{13c}$$

where $\pi_B^{eff} = r_1^{eff} - r_2^{eff}$ is the net consumption rate (Eq. (2b)) of either species B in the example of first-order series-reactions or of 1BE in the selective hydrogenation example. The definition of r_{ref} is a consequence of the stoichiometric and kinetic features of the examples. In both cases reaction 1 proceeds independently of reaction 2, but the occurrence of reaction 2 strongly depends on the first reaction. For the first-order series-reactions, the case with $C_{BS} = 0$ is relevant. When this condition is combined with small values of ϕ_1, very small values of C_B inside the catalyst arise. Consequently, r_2^{eff} will be very low and, in practice, negligible. Thus, if the low value of r_2^{eff} were used as the reference rate in Eq. (13b), large values of ε_2 could arise, but without any practical significance. On the other hand, when continuously varying the values of the system parameters (ϕ_1, ϕ_2, C_{BS}/C_{AS}), a value $\pi_B^{eff} = 0$ will arise and therefore π_B^{eff} cannot be used indiscriminately as a reference rate in Eq. (13b). The choice of r_{ref} in Eq. (13b) eliminates the described singular situations and provides a significant evaluation from a practically point of view for the deviation of the 1D models. Basically the same pattern holds in the selective hydrogenation example, with BD reacting independently and 1BE playing the role of the intermediate product. Yet, even if $C_{1BE,S}$ is large, r_2^{eff} can still be very low, due to the strong inhibition effect exerted by the presence of BD. Consequently, r_{ref} defined in Eq. (13b) will be used for this example too.

By construction, the 1D models predict the correct values of r_j^{eff} either for very low or very high Thiele modulus. Therefore, the precision of the 1D-models can be conveniently assessed by identifying for each reaction j the error ε_j^{max} with a maximum absolute value in the whole range of Thiele moduli.

In Tables 3–6 introduced in the following sections, the symbol $^{(*)}$ accompanying values of ε_j^{max} indicates that $r_{ref} = r_2^{eff}$ holds in Eq. (13b).

4.1. First order series-reactions

It was assumed the same value for the effective diffusivities of both species, A and B, in this example ($D_A = D_B = D$). Considering first the case with $C_{A,S} = 1$ mol/l and $C_{B,S} = 0$, two sets of results were obtained for the cross-section shapes defined in Table 1, either with finite heights ($b^* > 0$, Table 3) or when $H \to \infty$ ($b^* = 0$, Table 4). In each case, ϕ_1 (Eq. (12a)) was varied in the whole range of feasible values ($0 \leq \phi_1 \leq \infty$), while the values $\phi_2/\phi_1 = 0.1, 1, 10$ were used for the second reaction (Eq. (12b)). The results, in terms of ε_j^{max} are displayed in Tables 3 and 4.

Tables 3 and 4 show that the precision of the 1D-VD model is always better than 1% and that the errors from the use of the 1D-GC are bounded by 7% in both cases, using σ_γ (Eq. (4)) or σ_Γ (Eq. (5)) to define the shape parameter. These results indicate that any of the 1D models can be employed with quite acceptable precision. For the solid cylinder and trilobe, the errors are always very low and the 1D-GCΓ model can be conveniently used, on account of the simple evaluation of parameter Γ (Table 2). Table 4 for $b^* = 0$ shows errors from both models 1D-GCγ and 1D-GCΓ somewhat larger than in Table 3, according to the expectation that long cylinders usually introduce larger discrepancies.

The solid cylinder with $b^* = 0$ was not considered in Table 4 as in this case any of the 1D-GC models (1D-GCγ or 1D-GCΓ) are exact while the 1D-VD produces negligible errors.

It is recalled that the reaction 1 ($A \to B$, $r_1 = k_1C_A$) proceeds independently of the second reaction and the values of ε_1^{max} correspond to those of a single first order reaction. Therefore, for the purpose of the present work, the values of ε_2^{max} are of particular significance. Tables 3 and 4 show that ε_2^{max} are only moderately higher than ε_1^{max}.

For the results of finite (Table 3) or infinitely long cylinders (Table 4) the values ε_1^{max} take place for intermediate values of ϕ_1 (between 0.5 and 3.5). The values ε_2^{max} take place when $\phi_1 = \phi_2$ and in the range $0.5 \leq \phi_1 \leq 4.5$. A typical behavior for the ratio $r_2^{eff}/r_{1,S}$ is illustrated in Fig. 1. The 1D-VD model reproduces very precisely all the data points evaluated for the actual pellet shape. The 1D-GC introduces some differences, especially around the maximum. As expected, the differences are more rapidly attenuated towards lower values of ϕ for the 1D-GCγ model and towards higher values for the 1D-GCΓ model. It should be noted that r_2^{eff} continuously increases as $\phi_1 = \phi_2$ does, but the ratio $r_2^{eff}/r_{1,S}$ plotted in Fig. 1 presents a maximum, due to the fact that diffusion limitations confine the presence of B to a narrow zone close to external surface when $\phi_1 = \phi_2$ is raised.

Two further sets of evaluations were carried out for $C_{B,S} \neq 0$ ($C_{B,S}$ [mol/l] = 0.5 and 1), while keeping $C_{A,S} = 1$ mol/l, for the 4-holed ring with $b^* = 0$. Then, for the sequence $C_{B,S} = (0, 0.5, 1)$ mol/l, the errors ε_2^{max} for the 1D-VD model were kept below 0.1% in all cases, while they follow the sequence $(-6.3, -5.1, -4.7)$ for the 1D-GCγ, and (7.3, 6.4, 5.6) for 1D-GCΓ. A slowly decreasing trend can be appreciated, in line with the fact that the raise of $C_{B,S}$ will ultimately turn the system into two reactions acting in parallel and independently of each other.

Table 3
Maximum errors ε_j^{max} in the prediction of effective reaction rates from 1D-models for first-order series reactions with finite heights ($b^* > 1$) of particle shapes defined in Table 1. $C_{A,S} = 1$ mol/l and $C_{B,S} = 0$. The symbol $^{(*)}$ indicates $r_{ref} = r_2^{eff}$ holds in Eq. (13c).

Model	Pellet (ε_1^{max}, ε_2^{max})				
	Solid cylinder		4-holed ring	Trilobe	Wagon wheel
	$b^* = 0.59$	$b^* = 2.5$	$b^* = 0.55$	$b^* = 0.86$	$b^* = 1.1$
1D-VD	0.4, 0.5	0.4, 0.6	0.1, 0.3	0.3, 0.5	0.3, 0.6
1D-GCγ	0.3, 0.4$^{(*)}$	0.4, 0.6	−3.3, −4.5	0.2, 0.3$^{(*)}$	−2.2, −2.9
1D-GCΓ	-0.5, -0.6$^{(*)}$	−1.4, −1.9	2.8, 4.1	−0.7, −0.8$^{(*)}$	0.5, 0.9

ralalical Engineering Journal 335 (2018) 876–886

Table 4
Maximum errors ε_j^{max} in the prediction of effective reaction rates from 1D-models for first-order series-reactions with infinite heights ($b^* = 0$) of particle shapes defined in Table 1. $C_{A,S} = 1$ mol/l and $C_{B,S} = 0$. The symbol $^{(*)}$ indicates $r_{ref} = r_2^{eff}$ holds in Eq. (13c).

Model	Pellet (ε_1^{max}, ε_2^{max})		
	4-holed ring	Trilobe	Wagon wheel
1D-VD	0.1, −0.1	0.1, 0.3	−0.2, −0.3
1D-GCγ	−4.3, −6.3	−0.3, −0.4	−3.5, −5.0
1D-GCΓ	4.9, 7.3	−0.4, −0.5	2.0, 2.8

Table 5
Values ε_j^{max} from the 1D-models for selective hydrogenation. $b^* = 0$ and base-case conditions (Eqs. (16)). The symbol $^{(*)}$ indicates $r_{ref} = r_2^{eff}$ holds in Eq. (13c).

Model	Pellet (ε_1^{max}, ε_2^{max})	
	4-holed ring	Trilobe
1D-VD	1.4, 2.2 $^{(*)}$	0.8, −1.3 $^{(*)}$
1D-GCγ	−6.3, 11.3 $^{(*)}$	0.2, 0.2
1D-GCΓ	12.1, 18.6 $^{(*)}$	−0.3, 0.3

Table 6
Values ε_j^{max} and $\delta_{j,GC}^{max}$ from the 1D-models for selective hydrogenation in a 4-holed ring ($b^* = 0$) for different conditions. The symbol $^{(*)}$ indicates $r_{ref} = r_2^{eff}$ holds in Eq. (13c).

Conditions	(ε_1^{max}, ε_2^{max})			
	1D-VD	1D-GCγ	1D-GCΓ	$\delta_{j,GC}^{max}$
Base case	1.4, 2.2 $^{(*)}$	−6.3, 11.3 $^{(*)}$	12.1, 18.6 $^{(*)}$	−13.3, 21.8
$y_{1BE,S} = 0$	1.8, −3.8	−6.4, 14.4	15.4, 22.4	−15.5, −19.6
$x_{H2,S} = 0.0025$	0.1, 0.0	−4.0, −0.3	−5.04, 0.4	−8.1, −0.6
$x_{H2,S} = 0.005$	−0.3, 0.4	−6.3, 2.6	7.8, 4.7	11.0, −4.2
$x_{H2,S} = 0.01$	0.7, −0.8	−6.7, 6.6	10.3, 13.2	−13.0, −10.6
$k_2 = 0.2k_1$	1.4, −0.3	−5.8, −1.4	12.1, −2.5	−12.4, 2.6
$k_2 = k_1$ (base case)	1.4, 2.2 $^{(*)}$	−6.3, 11.3 $^{(*)}$	12.1, 18.6 $^{(*)}$	−13.3, 21.8
$k_2 = 5k_1$	1.4, −6.2 $^{(*)}$	−6.0, −29.6 $^{(*)}$	12.0, −60.7 $^{(*)}$	−12.2, 78.8 $^{(*)}$
$k_2 = 20k_1$	1.3, 14.4 $^{(*)}$	−6.1, 39.0 $^{(*)}$	11.6, −60.4 $^{(*)}$	−12.8, 78.9 $^{(*)}$
$K_{BD}/K_{1BE} = 5$	0.4, 1.8 $^{(*)}$	−4.3, −6.7 $^{(*)}$	4.8, 13.5 $^{(*)}$	−7.4, −15.2 $^{(*)}$
$K_{BD}/K_{1BE} = 100$	0.5, −2.3 $^{(*)}$	−5.5, 7.4 $^{(*)}$	7.5, 16.5 $^{(*)}$	−10.3, 15.7 $^{(*)}$
$K_{BD}/K_{1BE} = 1000$ (base case)	1.4, 2.2 $^{(*)}$	−6.3, 11.3 $^{(*)}$	12.1, 18.6 $^{(*)}$	−13.3, 21.8
$K_{BD}/K_{1BE} = 10,000$				−13.0, 19.5

4.2. Selective hydrogenation

It was noted in Section 3 that the solution of Eqs. (1) for reactions (10) with kinetics defined in Eqs. (11) involves a large number of parameters. Some of them will be fixed here according to actual values of the variables for this example. The effective diffusivity of H_2 is about 4 times larger than those for BD and 1BE, which in turn are similar to each other [1]. Then, it was taken $D_{BD} = D_{1BE} = D$, $D_{H_2}/D = 4$. From $D_{BD} = D_{1BE}$, the ratio of Thiele moduli defined in Eqs. (12) becomes

$$\phi_2 = \phi_1 \sqrt{\frac{k_2}{k_1} \left(\frac{K_{1BE}}{K_{BD}} \right)} \tag{15}$$

The available experimental evidence indicates that the kinetic coefficient k_1 and k_2 are similar [1]. Following the kinetic expressions
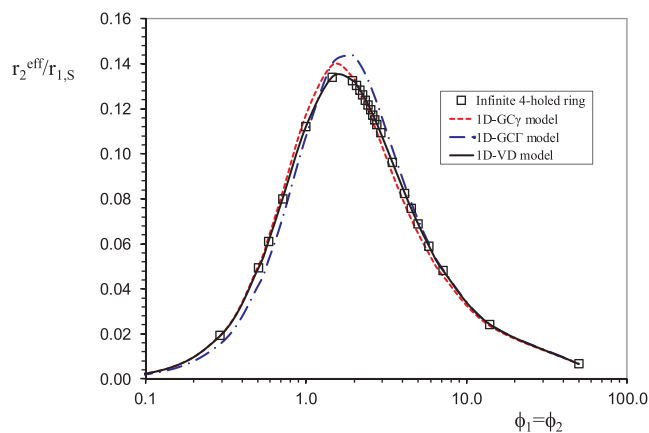

Fig. 1. $r_2^{eff}/r_{1,S}$ vs. ϕ (with $\phi_1 = \phi_2$) for first-order series-reactions in a 4-holed ring with $b^* = 0$. $C_{A,S} = 1$ mol/l and $C_{B,S} = 0$.

(11), this finding shows that both species, BD and 1BE, will react at a similar rate, $r_j = k_j y_{H2}$, when only one of them is present. To define a base set of conditions, $k_1 = k_2$ will be assumed. Besides, it was already commented on in Section 3 that the ratio K_{BD}/K_{1BE} reaches values around 1000. Therefore, $K_{BD}/K_{1BE} = 1000$ was first considered. These assumptions lead to $\phi_1 = 0.032\phi_2$ in Eq. (15). In turn, it has been checked that the range $0.01 < \phi_1 < 32$ was suitable to identify the maximum errors ε_j^{max}.

For the base set of conditions, it is assumed that $y_{BD,S} = 0.01$ and $y_{1BE,S} = 0.2$. These are typical values for a C4 cut.

The concentration of H_2 dissolved in the liquid phase is highly relevant for the selectivity of the process when BD is depleted inside the catalyst, due to diffusion limitations (high values of ϕ_1). Taking into account that $D_{H_2}/D_{BD} = 4$, if $y_{H_2,S} > y_{BD,S}/4$ there will be an excess of H_2 inside the catalyst after the extinction of BD. Therefore, 1BE will be free to adsorb and react with the H_2 surplus. To consider the worst possible scenario, as regards 1BE hydrogenation, it will be asumed for the base case that the molar fraction of H_2 remains uniform inside the catalyst pellet, i.e. $y_{H2} = y_{H2,S}$.

In summary, the conditions for the base case are:

$$D_{BD} = D_{1BE}; k_1 = k_2; K_{BD}/K_{1BE} = 1000; \tag{16a}$$

$$y_{BD,S} = 0.01; y_{1BE,S} = 0.2; y_{H2} = y_{H2,S} \tag{16b}$$

The set of values in (16) will be modified for the evaluations discussed in Section 4.2.4.

The results for this example will be limited to evaluations in the 4-holed ring and in the trilobe (Table 1). The 4-holed ring was chosen because it was the shape that introduced the largest deviations from the 1D-models in the example of first-order series-reactions (Tables 3 and 4). The trilobe was chosen as a reference shape on account of its use in commercial selective-hydrogenation processes (e.g. PRICAT PD 309/4 from Johnson Matthey). In addition, the case $b^* = 0$ ($H \rightarrow \infty$) was considered, as it also enhances the errors from the 1D-models.

4.2.1. Results for the base- case conditions

The values ε_j^{max} from the use of the 1D models are reported in Table 5. The errors from the 1D-VD model are bounded by 2% and therefore the results from this model are quite satisfactory. Instead, it is evident that both versions of the 1D-GC model show a lack of precision, particularly regarding ε_2^{max}, for the 4-holed ring. On the other hand, the three 1D models are highly precise for the trilobe pellet.

Fig. 2a,b show the effect of ϕ_1 and $\phi_2 = 0.032\phi_1$ on the errors ε_j (Eqs. 13). It can be appreciated that the 1D-VD model keeps very low errors ε_j in the whole range. It is also significant to note that although the values ε_j^{max} (Table 5) for the 1D-GCγ model are smaller than for the 1D-GCΓ model, relatively large values $|\varepsilon_j|$ are sustained even at large values of ϕ_1 for the 1D-GCγ model.
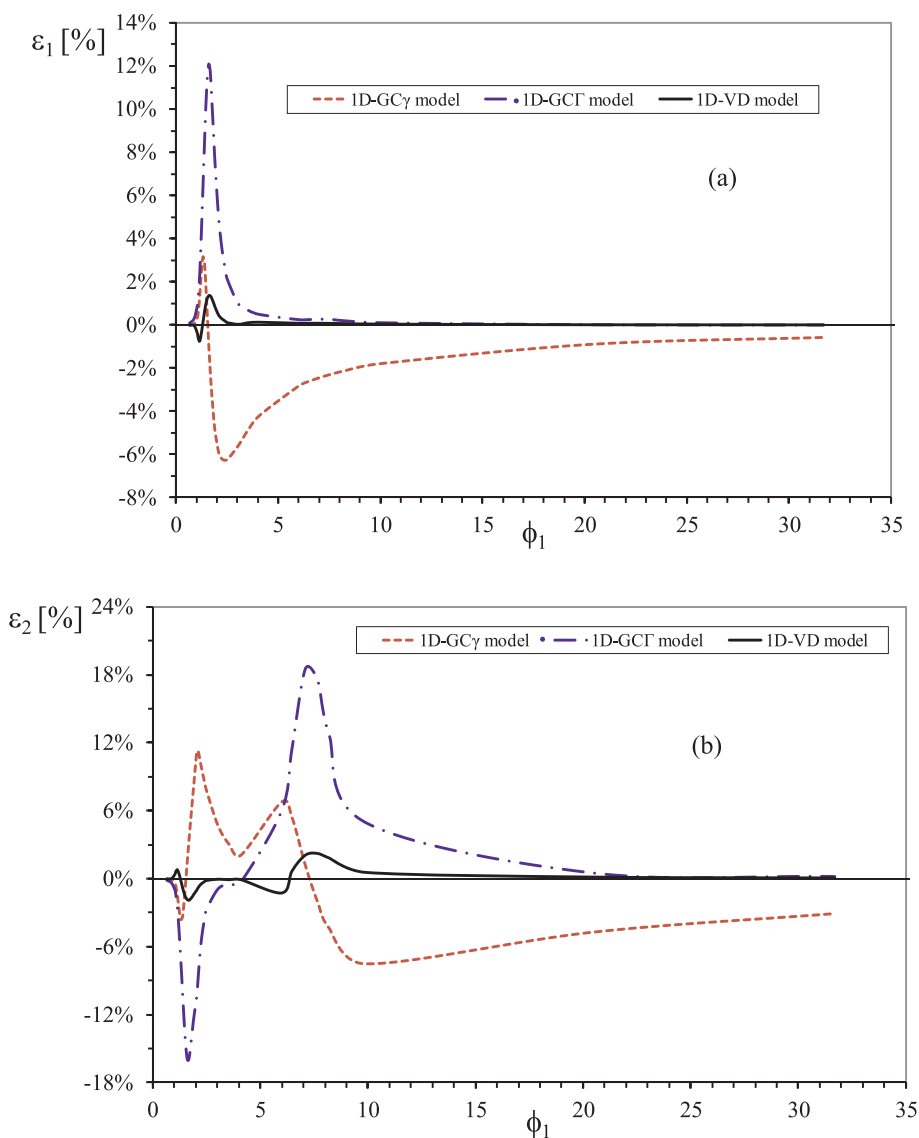
881

4.2.2. Analysis of errors

This section can be skipped in a first reading. Nonetheless, it is emphasized that it can provide an important insight about the sources of errors in the predictions and limitations of the employed 1D models.

By comparing the results in Table 5 with those in Table 4 (first-order series-reaction example) for the 4-holed ring, it becomes clear that the kinetic features of the selective hydrogenation case combined with some specific pellet shapes will enhance the appearance of higher levels of error from the 1D-models, of special practical significance for the 1D-GC model.

To explain the reasons for this behavior, the values of ϕ_1 at which the 1D-GCΓ model shows the peaks of ε_2 in Fig. 2b are chosen: $\phi_1 = 1.65$ ($\phi_2 = 0.05$) and $\phi_1 = 7.09$ ($\phi_2 = 0.2$). For these Thiele moduli, Fig. 3 shows for the 1D-VD and 1D-GCΓ models the profiles of molar fractions y_{BD} and y_{1BE} (Fig. 3a-I,II) and of hydrogenation rates ($r_1/r_{1,s}$) and ($r_2/r_{1,s}$) (Fig. 3b-I,II), where $r_{1,s}$ is very closely equal to the plateau value, $r_{1,s} = k_1 y_{H2,s}$. In these figures the coordinate $\zeta = V(z)/V_p = z^{(1+\sigma)}$ is used, where $\sigma = -0.94$ for the 1D-GCΓ model (Table 2) and $\sigma = 0$ for the 1D-VD model, to compare both models at the same volume. Note that $\zeta = 0$ is the pellet centre and $\zeta = 1$ the pellet surface.

As the errors from the 1D-VD model are small and roughly an order of magnitude less than those for the 1D-GCΓ model (Fig. 2), the results from the 1D-VD model will be supposed to be the "correct" ones and the

1D-GCΓ model plays the role of the "approximate" model.

In the case $\phi_1 = 1.65$, it can be appreciated in Fig. 3b,I that for the most part, the hydrogenation of BD proceeds almost independently of the 1BE hydrogenation and nearly as a zero-order reaction (i.e. close to the plateau value $r_1 = k_1 y_{H2,s}$). According to the 1D-VD model, only when the BD concentration has dropped to around a tenth of the surface value (Fig. 3a,I) 1BE starts reacting faster and even the plateau value $r_2 = k_2 y_{H2,s}$ (i.e., $r_2/r_{1,s} \approx 1$, as $k_1 = k_2$ in the base case) is reached close to $\zeta = 0$. Instead, Fig. 3a,I reveals that the 1D-GCΓ model does not predict the BD extinction and y_{BD} remains significantly greater than zero up to $\zeta = 0$, causing significant differences in the estimations of both, r_1 and r_2 (Fig. 3b,I), and consequently in the estimation of r_1^{eff} and r_2^{eff}.

The errors ε_j introduced by the 1D-GCΓ (Eqs. 13) can be approximately described by resorting to the limiting case $(K_{BD}/K_{1BE}) \to \infty$ and $\kappa = 0$ (Eq. (13c)). Thus, BD will strictly react as a zero order reaction, according to $r_1 = k_1 y_{H2,s}$, and 1BE will do so, according to $r_2 = k_2 y_{H2,s}$, but only after the point where $y_{BD} = 0$ is eventually reached. The situation is depicted in Fig. 4(I), where it is assumed that the BD disappearance occurs at a value ζ^{BD} near to $\zeta = 0$. In this way, the Eqs. (13) yield
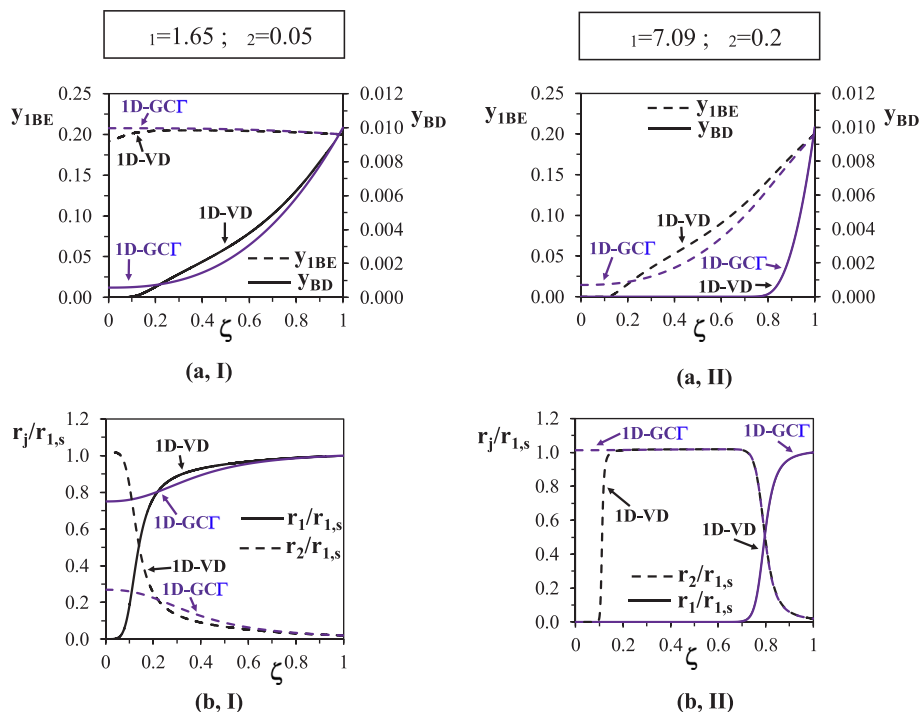
Fig. 3. Mole fraction (I) and reaction rate (II) profiles for selective hydrogenation using the 1D-GCΓ and 1D-VD models. 4-holed ring with $b^* = 0$ and base-case conditions (Eqs. (16)).

$$\varepsilon_1 = 100\frac{k_1(\zeta^{BD} - \zeta_{GC\Gamma}^{BD})}{k_1(1 - \zeta^{BD})} = 100\frac{(\zeta^{BD} - \zeta_{GC\Gamma}^{BD})}{(1 - \zeta^{BD})} \tag{17a}$$

$$\varepsilon_2 = 100\frac{k_2(\zeta_{GC\Gamma}^{BD} - \zeta^{BD})}{\max[k_1(1-\zeta^{BD}) - k_2\zeta^{BD}, k_2\zeta^{BD}]} = 100\frac{(\zeta_{GC\Gamma}^{BD} - \zeta^{BD})}{\max\left[\frac{1 - \zeta^{BD}}{(k_2/k_1)} - \zeta^{BD}, \zeta^{BD}\right]} \tag{17b}$$

where ζ^{BD} stands for the correct value and $\zeta_{GC\Gamma}^{BD}$ for the approximate value.

Eq. (17a) shows that ε_1 only depends on the ability of the approximate model to predict the location at which $y_{BD} = 0$ is reached. As deviations from the true concentration profile increase as the distance from the surface increases, relatively large values of ε_1 will arise when ζ^{BD} is close to zero. This behavior is at variance with that of a higher order reaction (e.g. a first order reaction), when ε_1 will depend on the whole concentration profile, and explains why ε_1^{max} becomes larger than in the example of first-order series-reactions.

From Eq. (17b), it is clear that ε_2 will be also conditioned to the correct prediction of ζ^{BD}. For the base case with $k_2/k_1 = 1$ and small values of ζ^{BD}, the denominator in Eq. (17b) becomes $(1-2\zeta^{BD})$, which corresponds to $r_{ref} = r_1^{eff} - r_2^{eff}$ (Eq. (13c)), and $\varepsilon_2 = 100(\zeta_{GC\Gamma}^{BD} - \zeta^{BD})/(1-2\zeta^{BD})$. By comparison with Eq. (17a), this expression tells us that values $|\varepsilon_2| > |\varepsilon_1|$ will arise.

Another relevant effect emerges from Eq. (17b). Assume a problem with a ratio (k_2/k_1) well above 1, such that the denominator in Eq.

(17b) will eventually turn out to be ζ^{BD}. Then, $\varepsilon_2 = 100(\zeta_{GC\Gamma}^{BD} - \zeta^{BD})/\zeta^{BD}$. If ϕ_1 is allowed to increase, a situation when $\zeta_{GC\Gamma}^{BD} = 0$ and $\zeta^{BD} \neq 0$ will arise for some value of ϕ_1, and the value $\varepsilon_2 = -100\%$ will be reached. This large error will take place even if the approximate model only introduces a slight retard in the disappearance of BD. Alternatively, the reverse situation with $\zeta_{GC\Gamma}^{BD} \neq 0$ and $\zeta^{BD} = 0$ can happen and then $\varepsilon_2 \rightarrow \infty$. Therefore, problems with large values of (k_2/k_1) will present an extreme parameter sensitivity, due to a combination of strong inhibition effects (by BD) on a very fast reaction (1BE hydrogenation), and large errors will arise from any geometric approximation. Actually, a small difference in the estimation of certain parameters, as effective diffusivities, will also introduce large errors even if the exact geometrical description is employed.

The second type of significant errors ε_2 can be discussed from Fig. 3a,II and b,II for the higher value $\phi_1 = 7.09$ ($\phi_2 = 0.2$). y_{BD} drops rapidly to zero and leaves a large fraction of pellet volume available for 1BE hydrogenation. It can be observed that for the 1D-VD model y_{1BE} drops to zero before the center of the pellet (Fig. 3a,II). Instead, the 1D-GCΓ model keeps $y_{1BE} > 0$ up to $\zeta = 0$ and a significant error ε_2 arises (actually, the largest value ε_2^{max} reported in Table 5 for the 1D-GCΓ corresponds to the situation in Fig. 3b,II). At this condition, $r_{ref} = r_2^{eff}$ (Eq. (13c)) for the base-case conditions.

For the limiting case $(K_{BD}/K_{1BE}) \rightarrow \infty$ (Sketch II in Fig. 4), the error ε_2 from Eq. (13b,c) becomes
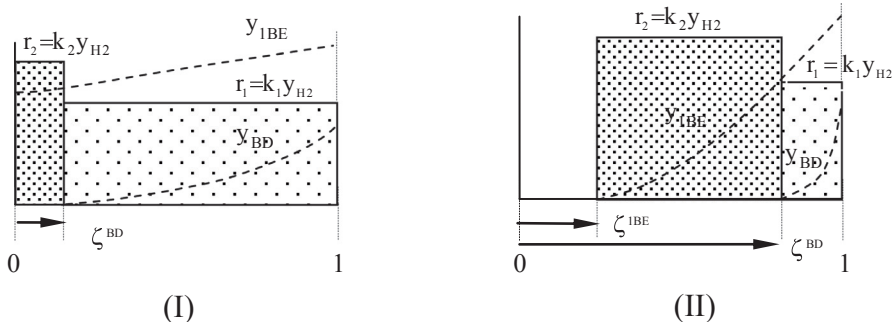

Fig. 4. Molar fraction and rate profiles when $(K_{BD}/K_{1BE}) \rightarrow \infty$. Sketch (I): $y_{BD} = 0$ is reached (intermediate value of ϕ_1). Sketch (II): $y_{BD} = 0$ and $y_{1BE} = 0$ are reached (large value of ϕ_1).

$$\varepsilon_2 = 100\left[\frac{\zeta_{GC\Gamma}^{BD}-\zeta_{GC\Gamma}^{1BE}}{\zeta^{BD}-\zeta^{1BE}}-1\right] \tag{17c}$$

where ζ^{1BE} stands for the position at which 1BE is extinguished. The error ε_2 in (17c) depends on the ability of the approximate model GCΓ to predict the correct size of the zone (ζ^{BD}-ζ^{1BE}) where 1BE reacts, which in turn depends on the precision of the estimates of both, ζ^{BD} and ζ^{1BE}. In this way, ε_2 can be expected to be larger than for the case of an isolated zero order reaction.

Errors ε_2 only related to the extinction of BD (Fig. 3a,b-I, intermediate values of ϕ_1) will be identified as type I errors and those that also involve the extinction of 1BE (Fig. 3a,b-II, relatively large values of ϕ_1) as type II errors. Fig. 2b reveals that for each 1D model there is a range of Thiele moduli in which ε_2 reaches significant levels. This range (approximately, $1.5 < \phi_1 < 8$) includes both type of errors for each 1D model. At lower values of ϕ_1, the error ε_2 drops very fast, but at higher values of ϕ_1 the error ε_2 decreases more slowly, at a rate depending on each model.

4.2.3. Computational issues

It is pertinent to note that severe convergence difficulties arise in the *Comsol Multiphysics®* platform when dealing with zero-order reactions at conditions leading to the extinction of the reactant somewhere inside the catalytic pellet and, therefore, the reaction rate profile becomes a step function. The problem can be circumvented by introducing a smoothed reaction rate, $r = k\,C_A/(\delta + C_A)$, solving the problem for a set of small values of δ and extrapolating the results to $\delta \to 0$. However, as small values of δ should be considered, the solver need a proper mesh refinement to obtain precision and achieve convergence. This strategy can be employed without many difficulties to solve 1D problems. For higher dimensions (2D or 3D problems), the choice of a balanced mesh to maintain precision and convergence under memory restrictions and/or keeping reasonable execution time becomes in our experience a major problem. Yet, as reported by Mariani et al. [14], it has been possible to tackle 2D problems, i.e. for infinitely long cylinders ($b^* = 0$) of different cross-section shapes, but the solution of the corresponding 3D problems ($b^* > 0$) could not be undertaken, for the most part.

For the present selective hydrogenation example, similar problems were faced for the base case parameters, as the reactions behave similarly as zero order reactions. In particular, the 4-holed ring could not be studied when considering a finite height. Also, values of the adsorption constant ratio (K_{BD}/K_{1BE}) significantly larger than 1000 could not be tried for the 2D case ($b^* = 0$). The need for employing a very refined mesh for (K_{BD}/K_{1BE}) = 1000 at values of ϕ_1 larger than the unit demanded long execution times to solve the example for 4-holed ring and $b^* = 0$, of the order of hours when performed on a standard PC. On the contrary, the solution of the 1D-models were reached in seconds. The large difference stresses the significance of reducing the dimension of the problem in the evaluation of effective reaction rates for multiple-reaction problems.

4.2.4. Results from modification of some variables from the base-case conditions

Since the largest values of ε_j^{max} are found for the 4-holed ring with $b^* = 0$ (Table 5), the effect of changing some variables or parameters from the values of the base-case (Eqs. (16)) will be considered here for that shape. Individual variations will be considered, while keeping the rest of values as for the base-case. The corresponding values of ε_j^{max}, which will be discussed below, are reported in Table 6 that also displays the values for the base case, for reference. In addition, Table 6 includes an evaluation of the differences between the 1D-GCγ and 1D-GCΓ models. Similarly to the errors ε_j (Eqs. 13), differences $\delta_{j,GC}$ are defined as

$$\delta_{1,GC} = 100\frac{r_{1,GC\gamma}^{eff}-r_{1,GC\Gamma}^{eff}}{r_{1,GC}^{eff}}; \tag{18a}$$

$$\delta_{2,GC} = 100\frac{r_{2,GC\gamma}^{eff}-r_{2,GC\Gamma}^{eff}}{\max\{r_{1,GC}^{eff}-r_{2,GC}^{eff},r_{2,GC}^{eff}\}} \tag{18b}$$

where $r_{j,GC}^{eff}$, is the average value from both models, 1D-GCγ and 1D-GCΓ. The difference $\delta_{j,GC}^{max}$ with a maximum absolute value in the whole range of Thiele moduli are reported in Table 6. The significance of $\delta_{j,GC}^{max}$ will be discussed in Sections 4.2.4.4 and 4.3.

4.2.4.1. Effect of the concentration of 1BE on the pellet surface.
Although the case $y_{1BE,S} = 0$ is not practically significant for actual operating conditions in the process of selective hydrogenation, it is of interest in kinetic studies when the hydrogenation of BD is intended to be isolated. For $y_{1BE,S} = 0$, the only source of 1BE is the hydrogenation of BD and 1BE is accumulated in the inner part of the pellet. The fraction y_{1BE} is anyway low and once BD is depleted, 1BE can be rapidly hydrogenated in a short distance. The maximum errors are of the type I defined above and they are only slightly larger than for the base case (Table 6).

4.2.4.2. Effect of the concentration of H_2 on the pellet surface.
The diffusion limitations of H_2 were suppressed for the base-case conditions. In practice, however, typical concentrations of dissolved H_2 are less than 1% (this corresponds roughly to about 10 bars of partial pressure) and therefore y_{H2} can diminish significantly inside the catalytic pellet. Three levels of $y_{H2,S}$ were considered to assess the impact of this variable on the precision of the 1D-models: $y_{H2,S} = (0.0025, 0.005, 0.01)$. The lowest level, $y_{H2,S} = 0.0025$, corresponds to the limiting value that allows the full consumption of BD inside the pellet, by recalling that $y_{BD} = 0.01$ for the base case and $D_{H2}/D_{BD} = 4$. Due to the H_2 limitation and the fact that both hydrogenation reactions are linearly dependent on y_{H2}, the reaction rates are faster close to the pellet surface. This effect explains that, in general, the errors made by the 1D models are lower the lower $y_{H2,S}$. Furthermore, due to the BD inhibition, the 1BE hydrogenation is mainly affected by the shortage of H_2, low values of r_2^{eff} arise and as a consequence of the definition of ε_2, considerable lower values of ε_2^{max} than for the base case are produced by every 1D model.

4.2.4.3. Effect of the kinetic coefficient ratio (k_2/k_1).
When the ratio (k_2/k_1) is changed, the ratio of Thiele moduli according to Eq. (15) becomes $\phi_2/\phi_1 = 0.032(k_2/k_1)^{0.5}$. Including the results for the base case, Table 6 displays the results for three values of (k_2/k_1): 0.2, 1, 5 and 20. As expected from the features of the present example, the ratio (k_2/k_1) shows practically no effect on ε_1^{max}, but a large impact is observed on ε_2^{max}. At the lowest value (k_2/k_1) = 0.2, type I errors prevail and the low values of r_2^{eff} lead to significantly lower values of ε_2^{max} than for the base case. For (k_2/k_1) = 5, the errors ε_2^{max} also correspond to type I, they take place in a tight range $1.4 < \phi_1 < 1.6$ for the three 1D models, but their values are substantially larger than for the base case. This situation occurs because k_2 is large enough to make $r_{ref} = r_2^{eff}$ (Eq. (13c)) in the definition of ε_2 and, therefore, very large type I errors arise, as it was advanced in Section 4.2.2 (it is recalled that in this case the approximate expression $\varepsilon_2 = 100(\zeta_{GC\Gamma}^{BD}-\zeta^{BD})/\zeta^{BD}$ applies). Comparing the values of ε_2^{max} for (k_2/k_1) = 5 and 20, it can be concluded that the 1D-GCΓ model has reached the maximum level of error, while the maximum level when (k_2/k_1) $\to \infty$ has not been reached for the 1D-VD and 1D-GCγ models. Two aspects should be stressed. First, the error ε_2^{max} of the 1D-VD model at the very high value (k_2/k_1) = 20 can be still acceptable. Second, it is recalled that if k_2/k_1 and K_{BD}/K_{1BE} are simultaneously raised, any approximate model will eventually produce values of $\varepsilon_2^{max} \to -100\%$ or $+\infty$, as it was discussed in Section 4.2.2.

4.2.4.4. Effect of the kinetic adsorption-constant ratio (K_{BD}/K_{1BE}).
Results

of ε_j^{max} for values of the ratio K_{BD}/K_{1BE} lower than in the base case are displayed in Table 6. The ratio $X = [(K_{BD}/K_{1BE})(y_{BD}/y_{1BE})]$ was introduced in section 3 to quantify the inhibition exerted by the presence of BD upon the 1BE hydrogenation. When evaluated at surface conditions $X = 1/4$ is obtained for $K_{BD}/K_{1BE} = 5$. This means that 1BE hydrogenation is barely inhibited by BD and, instead, the opposite effect is more important, although still moderate. BD and 1BE can react simultaneously with rates $r_1 \approx 5\,k_1 y_{H2}(y_{BD}/y_{1BE})$ and $r_2 \approx k_2 y_{H2}$, respectively. The errors ε_1^{max} are low and similar to those for a single first order reaction. The errors ε_2^{max} are noticeably lower than for the base case and correspond closely to that for a single zero order reaction [14].

For the intermediate ratio $K_{BD}/K_{1BE} = 100$, the inhibition of BD upon 1BE hydrogenation is already strong. The behavior of the system and consequently the errors ε_j^{max} approach those of the base case. The value ε_2^{max} corresponds in this case to type II errors.

As commented on in Section 4.2.3, the solution for the 4-holed ring could not be achieved for very large values of K_{BD}/K_{1BE}. Thus, there remains some uncertainty if values of K_{BD}/K_{1BE} higher than 1000 can modify the level of errors made by the 1D models. However, there are reasons to believe that values ε_j^{max} for the base case have approximately reached their highest levels, as regards the ratio K_{BD}/K_{1BE}. In first place, it is noted that the errors ε_1^{max} from the 1D models with $K_{BD}/K_{1BE} = 1000$ are already completely similar to those for a single zero order reaction [14], i.e. $K_{BD}/K_{1BE} = 1000$ allows approaching closely to the behavior as $K_{BD}/K_{1BE} \to \infty$, as concerns BD hydrogenation. Then, as the errors ε_2^{max} are strongly subject to BD hydrogenation (section 4.2.2), it can be expected that the limiting values of ε_2^{max} have been also approximately reached at $K_{BD}/K_{1BE} = 1000$. Furthermore, as results from the 1D models can be obtained for larger values of K_{BD}/K_{1BE} without numerical difficulties, the difference $\delta_{j,GC}$ (Eqs. 18) have been evaluated for $K_{BD}/K_{1BE} = 10,000$ (Table 6). It will be discussed in the next section that $\delta_{j,GC}^{max}$ quantifies with reasonable precision an upper bound for the errors ε_j^{max} of either the 1D-GCγ or the 1D-GCΓ model. The fact that the values of $\delta_{2,GC}^{max}$ for $K_{BD}/K_{1BE} = 1000$ and 10,000 are quite similar to each other, as shown in Table 6, provides further evidence that the error ε_2^{max} has reached very approximately its limiting value for $K_{BD}/K_{1BE} = 1000$.

4.3. The choice of a 1D model

The results discussed in Sections 4.1–4.2 and in previous contributions for single reactions [14,16] clearly show that the 1D-VD model is by far the most accurate and safest 1D model, particularly for rather singular shapes [16], for single reactions with a maximum rate inside the catalyst, due to thermal or self-inhibition effects [14] or due to an inhibition effect by other reactant, as in the selective hydrogenation example treated here. Nonetheless, the 1D-GC model will be accurate enough for a vast range of shapes and kinetics. Thus, for most 3D pellet shapes (e.g. cylinders with any cross-section shapes and finite heights) the 1D-GC model can be used safely for single reactions provided the "effective" reaction orders are non-negative [10]. The results presented here also indicate that the 1D-GC model can be used successfully for multiple reactions, as in the example of first-order series-reactions example or even for some conditions in the selective hydrogenation example.

The 1D-GC is believed to be more appealing than the 1D-VD model. Its single parameter σ keeps a clear geometric meaning in relation of the well known cases of a slab ($\sigma = 0$), an infinitely long cylinder ($\sigma = 1$) or a sphere ($\sigma = 2$). Also, the effectiveness factors for isothermal first order reactions can be expressed in terms of fractional-order modified Bessel functions of the first kind. Instead, the 1D-VD does not enjoy these features. Its parameters are introduced by means of locally dependent diffusion fluxes and they cannot be easily related to actual geometric properties. Although the evaluation of the three parameters does not involve a particularly complex numerical procedure, two of

them should be evaluated iteratively [16].

Having defined the pellet shape and the type of kinetics, a preliminary numerical study involving results for the actual pellet can be made to decide if the 1D-GC will provide an acceptable precision. However, as discussed in Section 4.2.3, obtaining a numerical solution for 2D or 3D problems may be at least laborious. Then, it can be useful to have a criterion to decide if the use of the 1D-GC can be suitable without having to carry out such a task. To this end, the difference $\delta_{j,GC}$ between both versions, 1D-GCγ and 1D-GCΓ, can be employed. It is shown in Table 6 that the values $\delta_{j,GC}^{max}$ very closely behave as an upper bound for the errors ε_j^{max} of either the 1D-GCγ or the 1D-GCΓ version. If $\delta_{j,GC}^{max}$ is large, say $> 25\%$, the use of the 1D-GC model can be ruled out. Provided $\delta_{j,GC}^{max}$ is tolerable, it cannot identify which version is better (clearly, in the selective hydrogenation example with the 4-holed ring and $b^* = 0$, the 1D-GCγ is more precise), but in our experience a combination $\sigma = 0.7\sigma_\gamma + 0.3\sigma_\Gamma$ is frequently suitable for using the 1D-GC model, if no further evidence is available.

Also, values of $\delta_{j,GC}^{max}$ can provide information for the precision of the 1D-VD model. Table 6 reveals that values of ε_j^{max} from the 1D-VD model are always less than $(1/5)$ of $\delta_{j,GC}^{max}$.

The information provided by $\delta_{j,GC}$ is not fortuitous. On one hand, $\delta_{j,GC}^{max}$ quantifies the loss of precision resulting for choosing either the high or low Thiele-moduli criterion to evaluate the parameter σ of the 1D-GC model. On the other hand, as the 1D-VD satisfies both limiting conditions, it can be reasonable expected that ε_j^{max} for this model can be estimated as a small fraction of $\delta_{j,GC}^{max}$.

5. Conclusions

The results obtained by the use of two geometric 1D models to approximate the behavior of 3D catalytic pellets when multiple reactions take place have been analyzed. One of models, identified as Generalized Cylinder (1D-GC) model, employs a single parameter that is either evaluated at the limit of low (1D-GCγ model) or high (1D-GCΓ model) reaction rates, while the second model, named Variable Diffusivity model (1D-VD), makes use of three parameters. Both models have been introduced in previous contributions and tested for single catalytic reactions. The precision of the 1D models was evaluated by comparing values of effective reaction rates with the results of solving the mass conservation equations on the actual geometry of four different pellet shapes: circular cylinder, trilobe, wagon wheel and 4-holed ring. The former two shapes are regarded as standard shapes, while the two later shapes were chosen because they proved to be a severe test for 1D models in the case of single reactions. The examples taken to check the precision of the 1D models are a system of first-order series reactions and the selective hydrogenation process of butadiene in the presence of 1-butene, in both cases under isothermal conditions. The examples were chosen because they lead to the existence of maximums in the rate of some of the reactions, somewhere inside the catalytic pellet. This poses a challenging feature for the 1D approximations, since the relevant maximum reaction rate cannot be identified beforehand and its magnitude and location will depend on properly predicting the concentration profiles inside the pellet.

In the example of first-order series reactions, the 1D-GC model produces maximum errors (identified by changing the Thiele moduli) in the estimation of the effective reaction rates of up to around 7%, which are regarded as being acceptable. A much better precision can be reached with the 1D-VD model, for which the errors kept below 1%.

The selective hydrogenation example was considered within the frame of the actual values of kinetic parameters. The hydrogenation of 1–3 butadiene (BD) on Pd catalysts proceeds closely as a zero-order reaction with respect to BD and the same happens for 1-butene (1BE) hydrogenation when BD is absent. However, BD strongly inhibits 1BE hydrogenation, a fact that introduces the main distinguishing feature of this example. Considering the usual range of composition, the 1D-GC model introduces errors of up to 20%, while the 1D-VD keeps errors

below 4%. A level of errors higher than in the first example is caused by the nonlinearity of the kinetics, in which the inhibition effect is of paramount significance. When the kinetic parameters of this example are freed to vary, the possibility of a rather singular behavior was identified. Thus, keeping the strong BD inhibition effect, but increasing the specific rate of 1BE hydrogenation, a large and thin peak of 1BE hydrogenation rate will appear in the innermost part of the pellet for some conditions. Any small deviation in the estimation of transport properties will cause a failure in evaluating, or not, such a peak. As a consequence, a geometric approximation for the pellet, regardless of how precise it may be, will inherit this feature and large and significant errors can appear.

This sort of cases, although believed to be infrequent in actual reaction systems, cannot be ruled out. Besides, it would be almost unaffordable trying to classify them in the frame of multiple reactions. It has been shown that employing and comparing both versions of the 1D-GC model (1D-GCγ and 1D-GCΓ) can provide a useful test to identify singular cases, as well as assessing its own level of precision.

Finally, it is worth remarking that, from a numerical point of view, the examples studied in this contribution revealed the significance of employing 1D approximations to deal with multiple reaction systems. Even when the actual pellet involves a 2D numerical solution, it frequently demanded a very careful setting of the calculation mesh, differences in computation time with respect to 1D evaluations of orders of magnitudes can arise and frequent convergence limitations were also faced in the course of the work here reported.

Acknowledgements

References

[1] J.A. Alves, S.P. Bressa, O.M. Martínez, G.F. Barreto, Kinetic evaluation of the set of reactions in the selective hydrogenation of 1-butyne and 1,3-butadiene in presence of n-butenes, Ind. Eng. Chem. Res. 52 (2013) 5849.

[2] R. Aris, A normalization for the thiele modulus, Ind. Eng. Chem. Fundam. 4 (1965) 227.

[3] B.A. Buffham, The size and compactness of particles of arbitrary shape: application to catalyst effectiveness factors, Chem. Eng. Sci. 55 (2000) 5803.

[4] A. Burghardt, A. Kubaczka, Generalization of the effectiveness factor for any shape of a catalyst pellet, Chem. Eng. Proc. 35 (1996) 65.

[5] R. Datta, S.W.K. Leung, Shape generalized isothermal effectiveness factor for first-order kinetics, Chem. Eng. Comm. 39 (1) (1985) 155.

[6] A.G. Dixon, D.L. Cresswell, Model reduction for two-dimensional catalyst pellets with complex kinetics, Ind. Eng. Chem. Res. 26 (1987) 2306.

[7] S.D. Keegan, N.J. Mariani, O.M. Martínez, G.F. Barreto, Behaviour of smooth catalyst at high reaction rates, Chem. Eng. J. 110 (2005) 41.

[8] S.D. Keegan, N.J. Mariani, O.M. Martínez, G.F. Barreto, Behaviour of catalytic pellets at high reaction rates. The effect of the edges, Ind. Eng. Chem. Res. 45 (2006) 85.

[9] J.P. Lopes, S.S.S. Cardoso, A.E. Rodrigues, Effectiveness factor for thin catalytic coatings: improved analytical approximation using perturbation techniques, Chem. Eng. Sci. 71 (2012) 46.

[10] N.J. Mariani, C. Mocciaro, S.D. Keegan, O.M. Martínez, G.F. Barreto, Estimation of effectiveness factor for arbitrary particle shape and non-linear kinetics, Ind. Eng. Chem. Res. 48 (3) (2009) 1172.

[11] N.J. Mariani, S.D. Keegan, O.M. Martínez, G.F. Barreto, A one-dimensional equivalent model to evaluate overall reaction rates in catalytic pellets, Chem. Eng. Res. Des. 81A (2003) 1033.

[12] N.J. Mariani, S.D. Keegan, O.M. Martínez, G.F. Barreto, On the evaluation of effective reaction rates on commercial catalyst by means a one-dimensional model, Catal. Today 133–135 (2008) 770.

[13] N.J. Mariani, C. Mocciaro, S.D. Keegan, O.M. Martínez, G.F. Barreto, Evaluating the effectiveness factor from a 1D approximation fitted at high Thiele modulus: spanning commercial pellet shapes with linear kinetics, Chem. Eng. Sci. 64 (2009) 2762.

[14] N.J. Mariani, M.J. Taulamet, S.D. Keegan, O.M. Martínez, G.F. Barreto, Prediction of effectiveness factor using one-dimensional approximations for arbitrary pellet shapes and abnormal kinetics expressions, Ind. Eng. Chem. Res. 52 (2013) 15321.

[15] D.J. Miller, H.H. Lee, Shape normalization of catalyst pellet, Chem. Eng. Sci. 38 (1983) 363.

[16] C. Mocciaro, N.J. Mariani, O.M. Martínez, G.F. Barreto, A three parameter one-dimensional model to predict effectiveness factor for an arbitrary pellet shape with linear kinetics, Ind. Eng. Chem. Res. 50 (2011) 2746.

[17] Z.I. Önsan, A.K. Avci (Eds.), Multiphase Catalytic Reactors. Theory, Design, Manufacturing and Applications, John Wiley & Sons, Inc, 2016.

[18] D. Papadias, L. Edsberg, P. Bjornbom, Simplified method for effectiveness factor calculations in irregular geometries of washcoats, Chem. Eng. Sci. 55 (2000) 1447.

[19] J. Piña, D.O. Borio, Modelling and simulation of an autothermal reformer, Latin Am. Appl. Res. 36 (2006) 289.

[20] J. Piña, N.S. Schbib, V. Bucalá, D.O. Borio, Influence of the heat-flux profiles on the operation of primary steam reformers, Ind. Eng. Chem. Res. 40 (2001) 5215.

[21] J.-M. Schweitzer, S.C. Ferreira, T. Sozinho Development of a new multi-shape particle description strategy: from meshing to discrete resolution, 24th International Symposium for Chemical Reaction Engineering (ISCRE 24); Minneapolis June 12–15, 2016, Paper 169.

[22] M.J. Taulamet, Fenómenos de transporte y reacción química en lechos fijos. Influencia de la forma del relleno catalítico, Tesis Doctoral Universidad Nacional de La Plata, 2015.

[23] R.J. Wijngaarden, A. Kronberg, K.R. Westerterp, Industrial Catalysis. Optimizing Catalysts & Processes, Wiley VCH, Weinheim, 1998.